Unusual Binding Stoichiometries and Cooperativity Are Observed during Binary and Ternary Complex Formation in the Single Active Pore of **R67** Dihydrofolate Reductase, a D_2 Symmetric Protein†

Thomas D. Bradrick,‡ Joseph M. Beechem,§ and Elizabeth E. Howell*,‡

Department of Biochemistry, University of Tennessee, Knoxville, Tennessee 37996-0840, and Department of Molecular Physiology and Biophysics, Vanderbilt University School of Medicine, Nashville, Tennessee 37232-0615

Received January 29, 1996; Revised Manuscript Received July 1, 1996⊗

ABSTRACT: **R67** dihydrofolate reductase (DHFR) is an R-plasmid-encoded enzyme that confers resistance to the antibacterial drug, trimethoprim. This DHFR variant is not homologous in either sequence or structure to chromosomal DHFRs. A recent crystal structure of the active tetrameric species describes a single active site pore that traverses the length of the protein (Narayana *et al.*, 1995). Related sites (due to a 222 symmetry element at the center of the active site pore) are used for binding of ligands, *i.e.*, each half-pore can accommodate either the substrate, dihydrofolate, or the cofactor, NADPH, although dihydrofolate and NADPH are bound differently. Ligand binding in **R67** DHFR was evaluated using time-resolved fluorescence anisotropy and isothermal titration calorimetry techniques. Under binary complex conditions, two molecules of either NADPH, folate, dihydrofolate, or N10 propargyl-5,8-dideazafolate (CB3717) can be bound. Binding of NADPH displays negative cooperativity, binding of either folate or dihydrofolate shows positive cooperativity, and binding of CB3717 shows two identical sites. Any asymmetry introduced by binding of one ligand is proposed to induce the cooperativity associated with binding of the second ligand. Evaluation of ternary complex formation demonstrates that one molecule of folate binds to a 1:1 mixture of **R67** DHFR + NADPH. These binding results indicate a maximum of two ligands bind in the pore. A mechanism describing catalysis is proposed that is consistent with the binding results.

Dihydrofolate reductase (DHFR,[1] EC 1.5.12.3) reduces dihydrofolate (DHF) to tetrahydrofolate using NADPH as a cofactor. DHFR is important in folate metabolism as the reaction product, tetrahydrofolate, is required for the synthesis of thymidylate, purine nucleosides, methionine, and other metabolic intermediates. Efficient inhibition of DHFR results in blockage of DNA synthesis and consequent cell death.

Inhibition of bacterial DHFR by trimethoprim (TMP) is the basis for clinical treatment of numerous bacterial infections. Resistance to trimethoprim has been observed clinically and correlated with the production of novel DHFRs encoded by R-plasmids. Type II R-plasmid-encoded **R67** DHFR is of particular interest as it is unrelated genetically and structurally to chromosomal DHFRs.

A crystal structure of a dimeric form of **R67** DHFR was reported by Matthews *et al*. in 1986. More recently, the active tetrameric species has been crystallized as an apo enzyme and as a binary complex with folate (Narayana *et al.*, 1995). From the refined structures, it is clear that the overall protein structure of **R67** DHFR is entirely different from that of chromosomal DHFR. Difference Fourier maps describing bound folate indicate the active site is a pore traversing the length of the molecule. One pore exists per tetramer and residues from each monomer contribute to binding. While a shared active site between protomers is not surprising, only one active site per oligomer is unusual.

The active site pore possesses exact 222 symmetry (D_2 symmetry where three 2-fold axes intersect at the middle of the tetramer). Therefore **R67** DHFR must bind ligands in an unusual manner. The difference Fourier map describing binding of folate to tetrameric **R67** DHFR shows electron density for the pteridine ring in the pore. If there is one binding site for folate, then from the 222 symmetry, there must be four binding sites. However due to steric constraints, it is unlikely that four ligands can bind concurrently. Fitting of the electron density describing bound folate indicates two asymmetric binding sites, Fol I and Fol II; each is present at $^1/_4$ occupancy due to the symmetry averaging of the binding sites (Narayana *et al.*, 1995). Fol I binds near the center in one half of the pore, while Fol II binds further out in the other half of the pore. A model for catalysis proposes the nicotinamide ring of cofactor NADPH binds near the center of the pore and reduces Fol I. This model suggests **R67** DHFR uses related sites (due to 222 symmetry) for binding of ligands, *i.e.*, *each half-pore can accommodate either DHF or NADPH*. However, DHF and NADPH are bound in different orientations.

Since the active site geometries in **R67** DHFR and *Escherichia coli* chromosomal DHFR are quite dissimilar,

† This research was supported by NIH Grants GM35308 (to E.E.H.) and GM45990 (to J.M.B). J.M.B. is a Lucille Markey Scholar in Biomedical Sciences.

‡ University of Tennessee.

§ Vanderbilt University School of Medicine.

⊗ Abstract published in *Advance ACS Abstracts,* August 15, 1996.

[1] Abbreviations: DHFR, dihydrofolate reductase; TMP, trimethoprim; DHF, dihydrofolate; NADP(+/H), nicotinamide adenine dinucleotide phosphate (oxidized/reduced); MTA buffer, 100 mM Tris + 50 mM MES + 50 mM acetic acid + 10 mM β-mercaptoethanol polybuffer; ITC, isothermal titration calorimetry.

S0006-2960(96)00205-X CCC: $12.00

numerous questions arise concerning catalytic function in **R67** DHFR. Are any special kinetic characteristics associated with the high degree of symmetry in the active site pore? What is the binding stoichiometry for cofactor and substrate under binary and ternary complex conditions? Is there any cooperativity in binding? This study addresses these questions.

MATERIALS AND METHODS

Steady State Kinetics. Steady state kinetic data were obtained with a Perkin-Elmer λ3a spectrophotometer interfaced with an IBM PS2 according to Howell *et al.* (1987). The computer program UVSL3 (Softways, Moreno Valley, CA) was used to collect and analyze data. Assays were performed at 28 °C in a polybuffer containing 50 mM acetic acid + 50 mM MES + 100 mM Tris + 10 mM β-mercaptoethanol (MTA). This buffering system maintains a constant ionic strength between pH 4.5 and 9.5 (Ellis & Morrison, 1982). Nonenzymic hydrolysis rates were measured and subtracted from enzymic rates. Inhibition studies were performed according to Segal (1975).

Protein and ligand concentrations were determined spectrophotometrically. In the case of **R67** DHFR, an extinction coefficient of 1.75 mL mg^{-1} cm^{-1} at 280 nm as determined by biuret assay (Gornall *et al.*, 1949) was used. Ligand concentrations were determined using the following extinction coefficients: 28 000 M^{-1} cm^{-1} at 282 nm for DHF and folic acid (Blakley, 1960); 6220 M^{-1} cm^{-1} at 340 nm for NADPH (Horecker & Kornberg, 1948) and 18 000 M^{-1} cm^{-1} at 259 for $NADP^+$ (Williams & Morrison, 1992). The molar extinction coefficients used to assess DHFR reduction of folate and DHF were 18 400 M^{-1} cm^{-1} (Hillcoat & Blakley, 1966) and 12 300 M^{-1} cm^{-1} (Baccanari *et al.*, 1975), respectively.

N10 propargyl-5,8-dideazafolate (CB3717), a folate analog, was the generous gift of Dr. Dave Matthews, Agouron Pharmaceuticals (San Diego, CA). Its concentration was determined spectrophotometrically in 0.1 N NaOH using an extinction coefficient of 23 700 M^{-1} cm^{-1} at 284 nm (Jones *et al.*, 1981).

Time-Resolved Fluorescence Anisotropy. Time-resolved experiments were employed to determine binding stoichiometries and to monitor the intrinsic fluorescence of either NADPH, DHF, or protein. 2 μL aliquots of ligand were added to 160 μL of MTA buffer (pH 8.0) containing 100 μM **R67** DHFR (tetramer), and time-resolved measurements were performed in 3 mm × 3 mm cuvettes. NADPH, DHF and folate concentration ranges were 10−300, 20−440, and 20−360 μM, respectively. For NADPH and DHF fluorescence, a 1 ps excitation beam at 327 nm was generated from a frequency-doubled Coherent 702 dye laser using Kiton Red dye synchronously pumped by a Nd:YAG laser (Coherent Antares). The emission signal was passed through a Glan-Thompson Polarizer, SPEX 0.22 m monochromator set at either 425 nm (DHF) or 450 nm (NADPH) and detected by a 6 μm microchannel plate detector (Hamamatsu, model R2809U) operating in single photon-counting, time-correlated mode. Tryptophan fluorescence utilized the same system but with Rhodamine 6G dye, which after frequency doubling produced 295 nm excitation; emission was monitored at 360 nm. The detection electronics were composed of a Phillips Scientific 2.5 GHz amplifier (Mahwah, NJ), a Tennelec (Oak Ridge, TN) constant fraction discriminator (TC455), a time to amplitude converter (TC862), and a Nucleus pulse-height analysis analog to digital converter (MIS3-8K). The stop pulse was obtained from an Antel (Burlington, Ontario, Canada) fast photodiode and constant fraction discrimination channel (TC455). Typical impulse response functions taken on water were 60−80 ps. During acquisitions, the emission polarizer rotated from vertical to horizontal every 30 s (ISS Koalo unit, Urbana, IL). Data sets consist of signal averaged data from 30 to 120 acquisitions of vertically or horizontally polarized emissions. Instrument *G* factor (polarization bias) was determined by rotating the excitation beam to the horizontal position and acquiring signal-averaged data for 15−30 s periods for both horizontal or vertical polarized emissions. Fluorescence lifetimes and correlation times were obtained by simultaneous fitting of the vertical and horizontal emission decay curves from each sample using the Globals Unlimited software package (Beechem *et al.*, 1991).

Fractional intensity plots were calculated in which the intensity is the product of the lifetime and amplitude terms and the components are constrained to sum to one. The breakpoints in the titration plots were calculated by comparing the correlation coefficients of a series of lines, where each successive line included additional data points. The lines with the best correlation coefficients were then utilized to define the breakpoint between the plateau and titration regions.

Isothermal Titration Calorimetry. Binding affinities, stoichiometries, and heats of binding were determined using isothermal titration calorimetry. Measurements were carried out on a Microcal Omega Ultrasensitive Isothermal Titration Calorimeter (Northampton, MA) equipped with a nanovoltmeter for improved sensitivity and connected to a circulating water bath for below-ambient-temperature operation. The data were collected automatically by an IBM PC running DSCITC data acquisition software and were analyzed using Origin software, both provided with the instrument by Microcal. The design and operation of this instrument have been described by Wiseman *et al*. (1989). Details concerning data analysis may be found in Wiseman *et al*. (1989), Lin *et al*. (1991), and Merabet and Ackers (1995). The "*c*" values for the binding of the different ligands to each site [where "*c*" is the product of the macromolecule (here the **R67** DHFR tetramer) concentration and the association constant] were typically between 1 and 50, within the range where data can be analyzed to obtain accurate binding constants (Wiseman *et al.*, 1989). Except as otherwise noted, samples typically consisted of an approximately 100 μM solution of **R67** DHFR tetramer in MTA buffer, pH 8. (For those experiments in which DHF was the titrant, the buffer consisted of 10 mM Tris, 1 mM EDTA, pH 8.) Measurements were made at 28 °C, except for the ternary complex **R67** DHFR + NADPH + folate, where the experiments were performed at 13 °C to minimize catalysis. A minimum of two separate measurements was made for each titration. Addition of ligand to buffer only was performed to allow base line corrections.

Kinetic Simulations. To test the validity of the proposed binding model(s), simulations of the **R67** DHFR-catalyzed reduction of dihydrofolate to tetrahydrofolate were performed using the program KINSIM (Barshop *et al.*, 1983) running on a Silicon Graphics INDIGO 2 workstation. A catalytic mechanism was proposed, and K_d's for substrate, cofactor, etc. were entered. KINSIM then calculated sample absorbance at 340 nm as a function of time from the predicted

concentration of DHF or NADPH using an extinction coefficient of 12 300 M^{-1} cm^{-1} (Baccanari *et al.*, 1975). For each simulation, the initial (unliganded) protein concentration was set at 0.43 μM. For those simulations where the NADPH concentration was varied, the DHF concentration was initialized at 60 μM, ten times its reported K_m (Reece *et al.*, 1991). Similarly, for those simulations where the DHF concentration was varied, the initial NADPH concentration was set at 30 μM (ten times its K_m; Reece *et al.*, 1991). The ligand concentration was then varied between 3 and 150 μM, and rates were calculated from the slopes of the absorbance vs time graphs. Predicted values for k_{cat} and the K_m's for DHF and NADPH were obtained from fits of the Michaelis−Menten equation to the substrate vs velocity graphs, and the extent of substrate or cofactor inhibition associated with a particular mechanism was evaluated. It should be noted that in carrying out the KINSIM simulations, a single pathway (*i.e.*, **R67** DHFR + A ⇄ **R67** DHFR·A + A ⇄ **R67** DHFR· 2A), rather than branched paths, was used to describe the binding of either DHF or NADPH (ligand "A") to the two binding sites in the central pore of **R67** DHFR. Therefore, to account for statistical effects, macroscopic K_d's equal to one-half and twice the microscopic K_d's for the first and second ligand molecules, respectively, were used in the simulations.

RESULTS

Stoichiometry Studies Using Time-Resolved Fluorescence Anisotropy. Early studies by Uyeda and Rabinowitz (1963) indicated that dihydrofolate is weakly fluorescent at pH 8−9. This observation was confirmed in our present studies where binding of DHF to **R67** DHFR was monitored using time-resolved fluorescence anisotropy techniques. The time-resolved fluorescence decay of free DHF is complex, requiring the use of at least three exponentials for reasonable fitting. The mean lifetime of free DHF is approximately 40 ps (Figure 1A, single exponential analysis), and the time-resolved anisotropy of free DHF shows complete depolarization in less than 1 ns (Figure 1B).

DHF fluorescence is enhanced upon binding to **R67** DHFR. The mean lifetime (single exponential analysis) of bound DHF increases to 500 ps (Figure 1A). In a 1.6:1 mole: mole complex with **R67** DHFR, an anisotropy decay indicative of predominately bound DHF is obtained (Figure 1B). We have found that the DHF binding stoichiometry can be conveniently monitored using the fractional intensity associated with two dominant lifetime terms. A very short lifetime term (<100 ps) can be used as a marker for free DHF, while a lifetime component of approximately 320 ps describes bound DHF. Plotting these fractional intensities vs the ratio of DHF concentration to **R67** DHFR concentration clearly reveals two correlated titrations (Figure 1C). Bound DHF is the predominant species up to approximately 200 μM DHF; above this concentration, free DHF begins to accumulate and the average fluorescence lifetime decreases (Figure 1A). Fitting the free DHF term in Figure 1C yields a binding stoichiometry of 1.7 DHF molecules per tetramer while fitting the bound DHF term gives a stoichiometry of 2.2. A summary of all the time-resolved fluorescence anisotropy results is provided in Table 1.

Binding of folate was investigated by monitoring changes in protein fluorescence. The time-resolved fluorescence

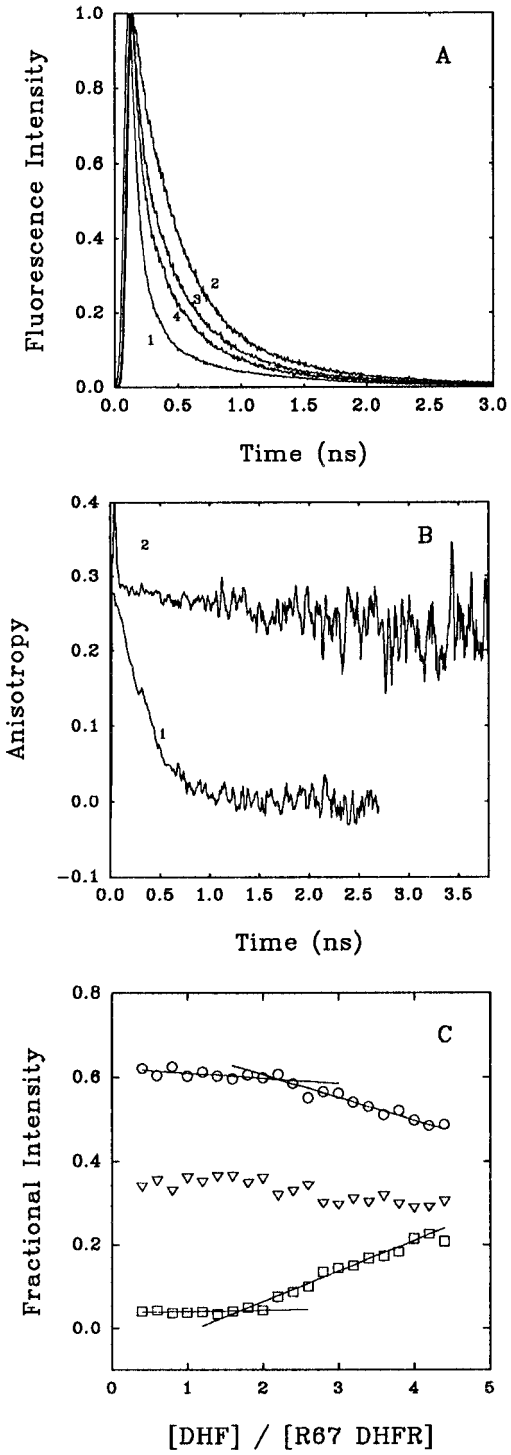

FIGURE 1: Time-resolved fluorescence total-intensity (panel A) and anisotropy data (panel B) for free and bound DHF at pH 8.0. (A) Normalized fluorescence total-intensity plots for free DHF and mixtures of 100 μM **R67** DHFR with 160, 300, or 400 μM DHF (curves 1−4, respectively). (B) Time-resolved anisotropy curves for free DHF and a mixture of 100 μM **R67** DHFR with 160 μM DHF (curves 1 and 2, respectively). (C) The lifetime curves were fit as described in the text and the fractional intensities for a short-lifetime term (<100 ps, □ points) and a long-lifetime term (approximately 320 ps, ○ points) were plotted as a function of [DHF]/[**R67** DHFR]. A third lifetime component was also obtained (▽ points, 0.9−1.8 ns lifetime range); however, the fractional change in its intensity was minimal and therefore not fit.

decay of W38 and W45[2] residues and their symmetry-related partners, W138,W238,W338,W145,W245,W345 in **R67** DHFR, requires the use of at least two exponentials for a good fit. An initial titration of protein fluorescence

Table 1: Binding Stoichiometry Studies Using Time-Resolved Fluorescence Data

complex	binding stoichiometry per tetramer	protein or ligand fluorescence monitored	K_d
binary			
100 μM **R67** DHFR, titrate with NADPH	0.8 NADPH	NADPH	2 μM[a]
100 μM **R67** DHFR, titrate with $NADP^+$	no titration observed	protein	nd[b]
100 μM **R67** DHFR, titrate with folate	saturation not reached	protein	nd
100 μM **R67** DHFR, titrate with DHF	1.95 DHF	DHF	nd
ternary			
100 μM **R67** DHFR + 200 μM NADPH, titrate with folate	1.0 folate	protein	K_i = 16 μM
100 μM **R67** DHFR + 300 μM folate, titrate with NADPH	1.0 NADPH	protein	nd
100 μM **R67** DHFR + 100 μM $NADP^+$, titrate with DHF	0.95 DHF	DHF	nd
100 μM **R67** DHFR + 200 μM NADPH, titrate with $NADP^+$	no titration observed	protein	nd

[a] From Zhuang *et al.* (1993). [b] nd, not determined.

describing folate binding can be observed although a plateau region is never reached when the amplitudes for two dominant lifetime terms (approximately 1.6 and 0.8 ns) are analyzed versus the ligand to tetramer molar ratio (data not shown). This result is consistent with weak binding of folate such that saturation does not occur under these binary complex conditions.

Steady state fluorescence quenching data has previously allowed calculation of a 1.1 NADPH per tetramer binding stoichiometry and a K_d value (2.0 μM) for **R67** DHFR using 2 μM tetramer (Zhuang *et al.*, 1993). Time-resolved fluorescence anisotropy measurements were used to investigate the NADPH binding stoichiometry at a higher enzyme concentration (100 μM). The time-resolved fluorescence decay of free NADPH is complex, requiring the use of at least two exponentials for a good fit (Visser & Van Hoek, 1981; Farnum *et al.*, 1991). The mean lifetime of free NADPH is approximately 0.34 ns, while the mean lifetime for NADPH bound to **R67** DHFR is 1.5 ns (data not shown, single exponential analysis). Figure 2A shows a time-resolved fluorescence anisotropy decay for free NADPH as well as for a mixture of 100 μM **R67** DHFR plus 50 μM NADPH. When the NADPH concentration is increased to 200−300 μM, an associative decay pattern is observed (Figure 2A). An associative decay curve superimposes a short-lifetime fast rotator with a longer-lifetime slow rotator (*i.e.*, bound ligand; Ludescher *et al.*, 1987). In other words, at low NADPH concentrations, the majority of the ligand is bound; however, at high NADPH concentrations, the observed steady state anisotropy decreases due to an increasing contribution from free NADPH. To evaluate the stoichiometry of NADPH binding, we calculated steady state anisotropy values and plotted them versus NADPH concentration. An effective binding stoichiometry of 0.80 NADPH per tetramer is obtained (Figure 2B).

To potentially extract more information from the data, we tried fitting the NADPH anisotropy curves using associative-type analyses; however, good fits were not obtained. An alternate explanation of the curves may be that if a second NADPH is bound, homotransfer (energy transfer between identical fluorophores; Runnels & Scarlata, 1995) causes the observed decreasing anisotropy (see isothermal titration calorimetry results and Discussion below).

[2] The amino acids in the first monomer are labeled 17−78; those in the second monomer, 117−178; those in the third monomer, 217−278; and those in the fourth monomer, 317−378. For brevity, when a single residue is mentioned in the text, all four symmetry equivalent residues are implied.

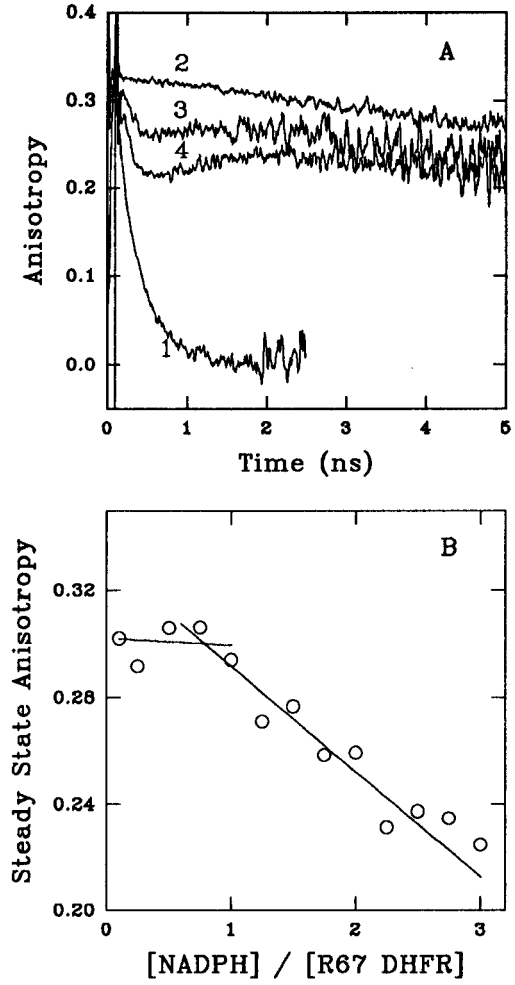

FIGURE 2: Time-resolved fluorescence anisotropy data for free and bound NADPH at pH 8.0. (A) Anisotropy curves describing free NADPH and mixtures of 100 μM **R67** DHFR with 50, 200, or 300 μM NADPH (lines 1−4, respectively). Lines 3 and 4 show an associative decay pattern (Ludescher *et al.*, 1987). (B) Steady state anisotropy values were calculated from the time-resolved data and plotted versus [NADPH]/[**R67** DHFR] to obtain the binding stoichiometry.

Since $NADP^+$ is not fluorescent, binding of oxidized cofactor was also attempted by monitoring the quenching of protein fluorescence. However, when 100 μM **R67** DHFR was titrated with $NADP^+$ (0−140 μM range), no obvious titrations were observed. From inhibition studies, we find that $NADP^+$ is a linear competitive inhibitor of NADPH (K_i = 30 μM; 0−208 μM range) under saturating DHF conditions (data not shown).[3] Either the protein fluorescence is not sensitive to binding of $NADP^+$ and/or the K_d is high

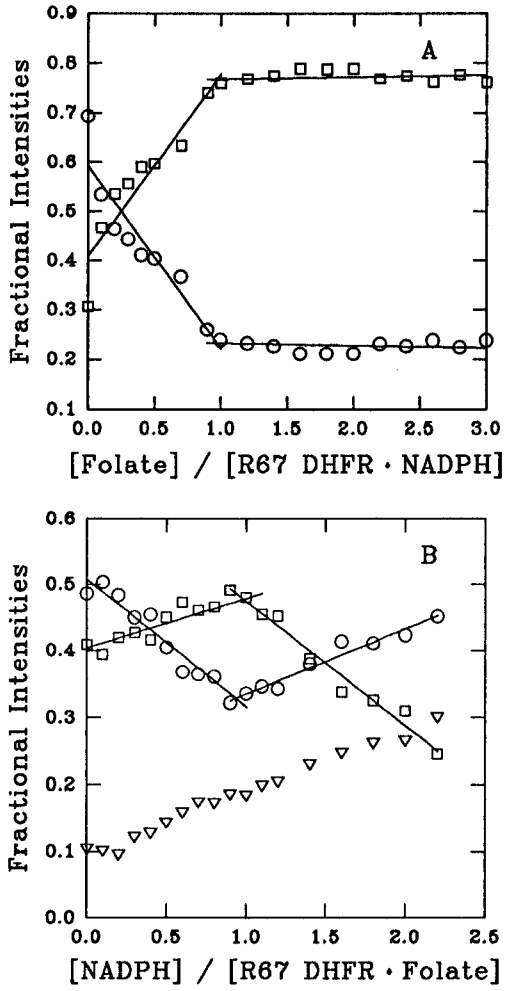

FIGURE 3: Ternary complex formation studied using time-resolved fluorescence. (A) A mixture of 200 μM **R67** DHFR + 200 μM NADPH (pH 8.0) was titrated with increasing concentrations of folate; the resulting protein lifetime curves were fit as described in the text. The fractional intensities display folate concentration dependence; ○ and □ points correspond to the 0.2−1.6 and 2−5 ns lifetime terms, respectively. Best fit values are given in the text. (B) Ternary complex formation studied using a mixture of 100 μM **R67** DHFR + 300 μM folate (pH 8.0). Increasing concentrations of NADPH were added, and the protein lifetime curves were fit. Two fractional intensity terms show an NADPH concentration dependence; ○ and □ points correspond to the 0.3−0.9 and 1.4−1.9 ns lifetime terms. A third fractional intensity term (▽ points, 0.05−0.15 ns lifetime range) is shown, but no obvious titration occurs.

under binary complex conditions and cannot be readily measured.

The above stoichiometry experiments describe only binary complex formation. To determine how many ligands are bound in a ternary complex with **R67** DHFR, we titrated increasing concentrations of folate into a mixture of 200 μM tetramer + 200 μM NADPH. As $n = 1$ for NADPH under these conditions, the initial population should be **R67** DHFR•NADPH. A plot of the normalized intensities associated with two lifetime terms (approximately 0.2−1.6 and 2−5 ns ranges) shows two correlated titrations (Figure 3A). An obvious breakpoint in each titration is observed at 1.0 folate bound per **R67** DHFR•NADPH, indicating that a total

[3] Previously Morrison and Sneddon (1990) reported that $NADP^+$ displays parabolic uncompetitive inhibition with respect to DHF. No K_i values or concentration ranges were reported. We have not examined the inhibition pattern using subsaturating DHF conditions.

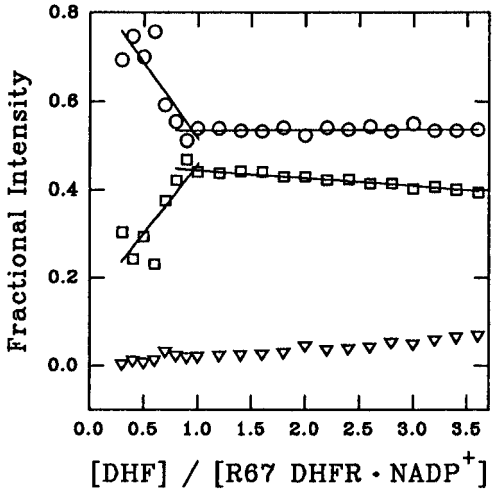

FIGURE 4: Time-resolved fluorescence measurements of DHF binding to a mixture of 100 μM **R67** DHFR + 100 μM $NADP^+$. DHF fluorescence was measured directly. Two fractional intensities display DHF concentration dependence; the ○ and □ points correspond to the 1−3 and 0.4−0.5 ns lifetime terms. A third fractional intensity term (▽ points, 0.02−0.14 ns lifetime range) with no obvious titration is shown.

of two different ligands are bound. Since our binary folate binding study did not show saturation, while this ternary complex titration does, it is probable that binding cooperativity exists between NADPH and folate. This hypothesis is further supported by our isothermal titration calorimetry results presented below.

Folate was used in the above ternary complex experiment (rather than DHF) as it is a very poor substrate; k_{cat} for folate reduction at pH 8, 20 °C, is 0.0036 min^{-1}. This rate may contribute to some minor catalysis during the titration curves, which take 2−3 h to complete. Two control points done within 5 min of each other at folate concentrations of 0 and 200 μM show the same relative position on the titration curve, consistent with a minimal contribution of catalysis to the binding curve.

We also performed the reverse experiment where a mixture of 100 μM **R67** DHFR + 300 μM folate was titrated with NADPH. Figure 3B shows the titration of two fractional intensities associated with two dominant lifetime terms. Protein fluorescence was monitored in this experiment, and while we do not understand the nonzero slopes, an obvious breakpoint in each titration is observed indicating a binding stoichiometry of 1.0 NADPH.

Two other ternary complexes were investigated. In one case, increasing concentrations of DHF were titrated into a mixture of 100 μM tetramer + 100 μM $NADP^+$. DHF fluorescence was monitored using the fractional intensities associated with two dominant lifetime terms. Plotting these fractional intensities vs DHF concentration reveals two correlated titrations (Figure 4). The two fractional intensity terms both appear to monitor bound DHF, as the fluorescent lifetimes are approximately 0.4−0.5 and 1−3 ns. An obvious breakpoint in each titration is observed at $n = 0.95$. Thus with equimolar concentrations of **R67** DHFR and $NADP^+$ present, the stoichiometry of substrate binding is decreased to only 1 DHF per tetramer. This result implies that 1 $NADP^+$ is bound per tetramer and prevents a second DHF molecule from binding. Since we were not able to monitor binary $NADP^+$ binding directly (above), to explain this result either $NADP^+$ binding must not produce a fluorescence change, or alternatively if the binary $NADP^+$

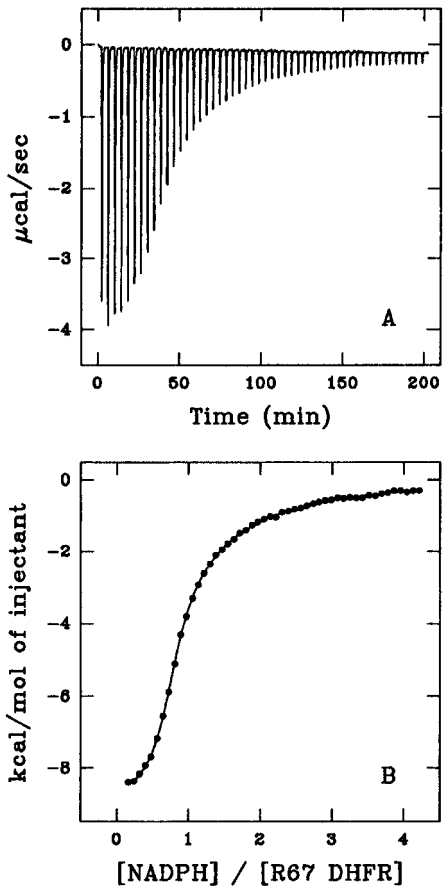

FIGURE 5: Binary complex formation between NADPH and **R67** DHFR at 28 °C as monitored by isothermal titration calorimetry. The initial protein concentration was 132 μM (tetramer). The top panel (A) shows the series of "peaks" that result from the heat liberated with each addition of NADPH as the cofactor is diluted and binds to the protein. As the protein approaches saturation, less of each subsequent addition is bound, so that the peaks decrease in height. The bottom panel (B) shows a plot of the heat liberated per mol of titrant added (the areas under the peaks in panel A divided by the number of moles of NADPH added) vs the cofactor/protein tetramer molar ratio. The smooth line shows the fit to the data for a model which describes ligand binding to two interacting sites which exhibit negative cooperativity. Average values for the stoichiometries, dissociation constants, and heats of binding are listed in Table 2. Note: the heat associated with the first peak in panel A was not included in panel B or in the analysis of the data.

K_d is high, then binding cooperativity must exist between DHF and $NADP^+$ for $NADP^+$ binding to occur in ternary complex conditions.

$NADP^+$ (0−440 μM range) was also added to a mixture of 100 μM **R67** DHFR and 200 μM NADPH. No evidence of a titration was observed when protein fluorescence was monitored.

While these time-resolved studies using high concentrations of **R67** DHFR indicate the binding stoichiometries under binary and ternary complex conditions, they do not yield K_d values and cannot indicate whether binding cooperativity exists. To answer these questions, we utilized a second independent technique.

Ligand Binding Monitored by Isothermal Titration Calorimetry. Isothermal titration calorimetry (ITC) measures the amount of heat released or absorbed upon ligand binding to a protein. Binding of NADPH to **R67** DHFR (average 95 μM tetramer) was monitored using this technique. The raw data shown in Figure 5A describe the heat evolved upon each injection of NADPH. The integrated heat *per injection* is shown in Figure 5B; this is not an additive value describing bound ligand as usually seen in binding curves. Fitting the data using a nonidentical-independent-sites model indicates 1.56 binding sites with a 38-fold difference in apparent or macroscopic K_d values. However, Bains and Freire (1991) have pointed out that ligand binding to two interacting sites which exhibit negative cooperativity is mathematically equivalent to binding to two nonidentical independent sites.[4] Since the crystal structure of tetrameric **R67** DHFR displays 222 symmetry consistent with symmetry-related ligand binding sites (Narayana *et al.*, 1995), we interpret the above ITC result as indicating that the binding of NADPH displays negative cooperativity. For data analyzed using an interacting sites model, K_2, the association constant for the second ligand molecule, is equal to kK_1, where K_1 is the association constant for the first ligand molecule and k is a cooperative interaction parameter. The k value describing NADPH binding is 0.106 ± 0.007, and the corresponding Δg (free energy of interaction $= -RT \ln k$) is 1.32 ± 0.04 kcal/mol. The stoichiometry as well as ΔH and K_d values for each site obtained using an interacting-sites model are listed in Table 2.

Here, as well as for the other ligands examined, the uncertainties were determined by the variation in the parameter values from experiment to experiment. (Note that the K_d's generated by the ITC fitting program are microscopic values; these are related to the macroscopic values by $K_{macro} = k_{micro}/2$ and $K_{macro} = 2k_{micro}$ for the first and second sites, respectively.) These NADPH binding results were initially surprising as the time-resolved fluorescence results above indicate only one binding site. However, homotransfer between two bound NADPH molecules could occur and result in a transfer depolarization term which would affect the calculated steady state anisotropy (see Discussion).

$NADP^+$ binding was monitored by ITC and only 1 weak binding site was observed with a K_d of 99 μM (data not shown). Using NMR, Brito *et al*. (1991) have previously monitored $NADP^+$ binding to RBG200 DHFR, an R-plasmid DHFR that is 78% homologous with **R67** DHFR. They find initial binding followed by a very slow isomerization. The K_d describing their isomerized complex is 1.9 mM ($n = 1$).

Addition of folate to **R67** DHFR shows an increase in heat released upon binding for several folate additions (Figure 6), consistent with positive cooperativity. The total number of folate sites is 2 with K_d's of 390 and 24 μM. Binding of DHF also displayed positive cooperativity (Figure 7), with 1.88 sites and K_d's of 250 and 4.4 μM. We note that for the **R67** DHFR tetramer concentrations typically used here (∼100 μM), the "*c*" values for the first folate and DHF sites are both somewhat less than unity. To potentially improve the accuracy of the first K_d values, we carried out titrations at ∼500 and ∼400 μM protein (for folate and DHF, respectively). For the folate titration, an increased noise in the early part of the titration (for which the injection volume was 2 μL to increase the number of data points in that region) made the value for the first K_d sensitive to changes in the base line and the value used for the protein concentration. Any fits of this data suggest, however, that the value for the first folate K_d could be up to twice that reported in Table 2.

[4] These authors were primarily concerned with analyzing calorimetric data obtained under conditions which result in extremely tight ligand binding (TAPS, total association at partial saturation). Such conditions did not obtain for our measurements.

Table 2: Results of Binding Studies Using Isothermal Titration Calorimetry

complex	binding stoichiometry per tetramer	K_d	$\Delta H_{binding}$ (cal mol^{-1})	no. of experiments
binary				
R67 DHFR with NADPH	1.56 ± 0.14	5.0 ± 0.3 μM	−8600 ± 200	2
		48 ± 2 μM	−5800 ± 2500	
R67 DHFR with NADP$^+$	0.99 ± 0.03	99 ± 3 μM	−7700 ± 500	2
R67 DHFR with folate	2.0	390 ± 10 μM	−1400 ± 500	2
		24 ± 2 μM	−11500 ± 50	
R67 DHFR with DHF	1.88 ± 0.1	250 ± 50 μM	−7900 ± 900	3
		4.4 ± 0.7 μM	−1400 ± 60	
R67 DHFR with CB3717	2.0 ± 0.03	2.2 ± 0.2 μM	−14500 ± 1500	2
ternary				
R67 DHFR + NADPH (1:1), titrated with folate[a]	0.87 ± 0.01	10.6 ± 0.4 μM	−8500 ± 500	2
R67 DHFR + NADP$^+$ (1:5), titrated with DHF	1.22 ± 0.01	4.8 ± 1.0 μM	−11700 ± 300	2
R67 DHFR + NADPH (1:1), titrated with NADP$^+$	0.82 ± 0.02	88 ± 8 μM	−6500 ± 800	2

[a] Titration of the binary **R67**·NADPH complex with folate was carried out at 13 °C to minimize catalysis. All the other calorimetric titrations were carried out at 28 °C.

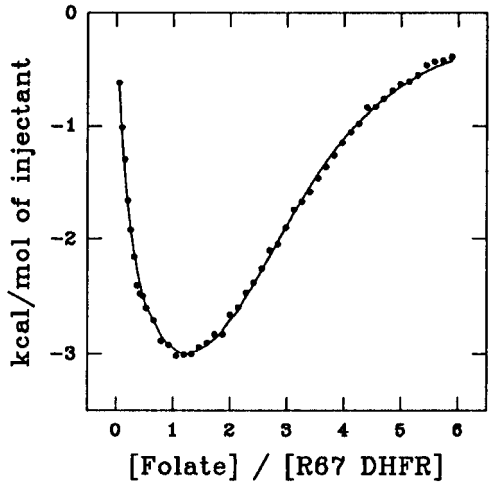

FIGURE 6: Binary complex formation between folate and **R67** DHFR at 28 °C as monitored by ITC. The total protein concentration was 105 μM (tetramer). The heat liberated per mol of titrant added is plotted vs the folate-to-**R67** tetramer molar ratio. These results indicate positive cooperativity as the amount of heat liberated with ligand binding initially increases up to a folate/**R67** tetramer molar ratio of about unity and then decreases. The smooth line shows the best fit to the data for a positively cooperative model with two binding sites. Best fit values are given in Table 2.

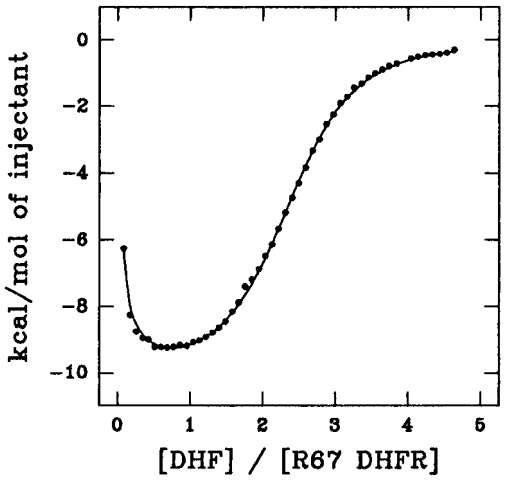

FIGURE 7: Binary complex formation between DHF and **R67** DHFR at 28 °C as monitored using ITC. The total protein concentration was 128 μM. The heat liberated per mol of DHF added is plotted vs the DHF-to-**R67** tetramer molar ratio. As seen for binding of folate to **R67** DHFR (Figure 7), the binding of DHF exhibits positive cooperativity (see Table 2 for fitted values).

For the titration with DHF, the ~12 mM DHF stock solution used in the titration was a suspension and the complication of a heat of solubilization caused problems in determining a more accurate value for the first K_d. In any case, we always observe the type of heat profiles shown in Figures 6 and 7, indicating positive cooperativity in the binding of these two ligands in their respective binary complexes.

Binding of N10 propargyl-5,8-dideazafolate (CB3717), a folate analog, was monitored, and 2.0 identical sites with a K_d of 2.2 μM (Table 2) were observed. [It was not necessary to invoke cooperativity in order to obtain a good fit to the data (not shown).]

Three ternary complexes were examined by ITC. First a 1:1 mixture of **R67** DHFR and NADPH was titrated with folate as shown in Figure 8. A binding stoichiometry of 0.87 folate was observed with a K_d of 11 μM (Table 2). This K_d is close to the second tight site observed under folate binary complex conditions (24 μM). The similarity between K_d values suggests folate binding displays positive cooperativity with either a previously bound folate *or* NADPH molecule. In a separate but related experiment we found that folate is a linear competitive inhibitor of DHF (K_i = 16 μM; 0−292 μM range) under saturating NADPH conditions (data not shown). This K_i value lies between the second binary folate K_d and the ternary folate K_d values given above.

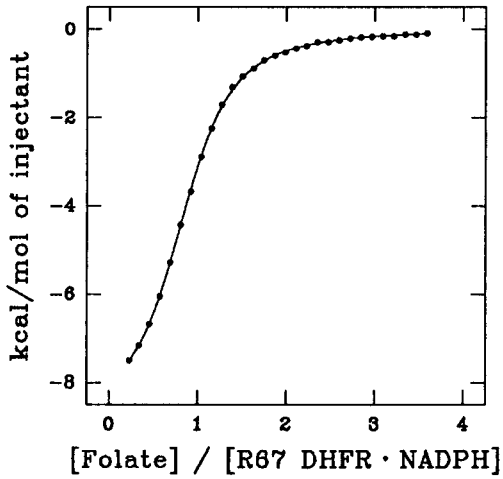

FIGURE 8: Ternary complex formation as monitored by ITC; a 1:1 mixture of **R67** DHFR and NADPH was titrated with folate. The initial protein concentration was 100 μM. Although folate is a poor substrate for **R67** DHFR, a limited amount of reduction of folate can take place. This experiment was therefore carried out at 13 °C to minimize catalysis.

A second ternary complex involved titrating DHF into a 1:5 mix of **R67** DHFR and $NADP^+$ (data not shown). 1.2 molecules of DHF were observed to bind (Table 2). Again, the observed K_d (4.8 μM) is similar to the second site K_d observed under DHF binary complex conditions (4.4 μM). This result suggests DHF binding displays positive cooperativity with either a previously bound DHF (binary) *or* $NADP^+$ molecule (ternary).

The last ternary complex monitored $NADP^+$ addition to a 1:1 mix of **R67** DHFR and NADPH. A K_d of 88 μM was observed ($n = 0.82$; data not shown).

It should be pointed out that the ITC data for the binary complex formed by **R67** DHFR with either NADPH, folate, or DHF was analyzed using a two-interacting-sites model to describe binding. As the Origin software package assumes integer stoichiometries in the case of interacting sites (*i.e.*, the stoichiometries are not treated as fitting parameters), adjustment of the sample concentration was sometimes necessary to optimize the fit. In the case of folate binding, however, no such adjustment was necessary for analyzing either of the two data sets for which average parameter values are reported in Table 2. The stoichiometry for the binding of that ligand is therefore given as 2, without any uncertainty (see Table 2). For the binding of DHF, the protein concentration had to be reduced by an average of about 6%, so that the stoichiometry is given as 1.88. For NADPH binding, a reduction in protein concentration of about 22% was necessary to obtain a good fit to the data. This result is consistent, however, with the stoichiometries obtained when the NADPH binding data are analyzed using a two-nonidentical-independent-sites model, in which case the software includes the stoichiometries as fitting parameters. (As pointed out above, ligand binding to two interacting sites which exhibit negative cooperativity is mathematically equivalent to binding to two nonidentical independent sites; Bains & Freire, 1991. From the latter analysis, stoichiometries of 0.80 ± 0.26 and 0.79 ± 0.10 are obtained for the first and second sites, respectively.)

DISCUSSION

Can Each Half of the Active Site Pore Accommodate either DHF or NADPH Binding? The active site pore in tetrameric **R67** DHFR possesses exact 222 symmetry. The pore is the active site as difference Fourier maps describing binding of folate to tetrameric **R67** DHFR show electron density for the pteridine ring in the pore and a protein concentration dependent pK_a (describing tetramer $\rightleftarrows$ 2 dimers) is observed in pH profiles of k_{cat} (manuscript in preparation). A proposed model for catalysis suggests the nicotinamide ring of cofactor NADPH binds near the center of the pore and reduces bound dihydrofolate/folate (Narayana *et al.*, 1995). In this model, **R67** DHFR uses related sites for binding of ligands and allows DHF and NADPH to be bound in different orientations/positions. Inhibition studies by Morrison and Sneddon (1990) are also consistent with different binding sites for DHF and NADPH as they find folate is a noncompetitive inhibitor of NADPH and $NADP^+$ is a parabolic uncompetitive inhibitor of DHF.

If there is one binding site for a ligand in the pore, then from the 222 symmetry operator, there must be four binding sites. Our binding studies indicate a maximum of two ligands can bind in the pore; apparently there is not enough room for four ligands to bind concurrently. From our binary complex studies described above, either 2 DHF *or* 2 folate *or* 2 CB3717 *or* 2 NADPH *or* 1 $NADP^+$ molecules can bind per tetramer. From the ternary complex studies, 1 NADPH + 1 folate *or* 1 $NADP^+$ + 1 DHF *or* 1 NADPH + 1 $NADP^+$ can bind concurrently. These results clearly support a model in which each half-pore can accommodate either DHF or NADPH. In other words, **R67** DHFR uses symmetry-related sites to bind either 2 NADPH or 2 folate molecules under binary complex conditions. However, under ternary complex conditions, there is only room for a total of two ligands as binding of only 1 folate is observed when titrated into a 1:1 **R67** DHFR:NADPH mixture. Therefore the folate binding stoichiometry is decreased from 2 to 1 molecules per tetramer going from binary to ternary complex conditions.

Cooperativity. From our binding data, it is clear that various ligands bind and interact differently. For example, under binary conditions, NADPH binding exhibits negative cooperativity; folate and DHF exhibit positive cooperativity; and CB3717 exhibits two identical sites. Changes in protein conformation do not occur upon binding as seen in a comparison of the crystal structure of the apo-enzyme with that of the binary folate·**R67** DHFR complex (Narayana *et al.*, 1995). Thus the observed cooperativity in binding is not due to an R $\rightleftarrows$ T (relaxed $\rightleftarrows$ tense) state equilibrium. Assuming that symmetry-related sites are being utilized during binding, the simplest way to obtain two different K_d values is to invoke interactions between the ligands themselves.

To explain the negative cooperativity observed in NADPH binding, NADPH likely binds near or through the center of the active site pore such that binding of a second NADPH molecule in a symmetry related site is impeded.[5] Either steric or electrostatic effects could be operating to weaken binding of the second NADPH molecule. Since folate binding exhibits positive cooperativity, the initial interaction of folate with **R67** DHFR must be weak and binding of a second folate molecule allows additional interactions with the first folate molecule. Finally, since binding of two CB3717 molecules does not display cooperativity, they must not interact with each other. The fact that negative, positive, and no cooperativity examples are observed with three different ligands supports a model where ligand−ligand interactions cause the cooperativity.

A similar case of negative cooperativity has previously been observed in binding of diphosphoglycerate (DPG) to the central pore of tetrameric deoxy hemoglobin. Only one DPG is bound near the symmetry axis, and binding of a second symmetry-related DPG is blocked due to overlapping sites (Arnone, 1972; Creighton, 1993).

Cooperativity is also observed in ternary complexes as the second, tighter K_d for binary folate binding (24 μM) is similar to the K_d for folate binding to the **R67** DHFR·NADPH complex (11 μM). Thus binding of folate is tight when either folate *or* NADPH is prebound.

DHF and $NADP^+$ also exhibit binding cooperativity as when DHF is titrated into a 1:5 mixture of **R67** DHFR:$NADP^+$, a tight K_d of 4.8 μM is observed for binding of 1

[5] It may not be as simple as this model, as perhaps binding of the second NADPH molecule concurrently weakens binding of the first NADPH molecule; see below KINSIM section. Additionally a Q67H mutant DHFR has been constructed, and this mutation affects both NADPH K_d values by a factor of 60 (Park *et al.*, manuscript in preparation).

Scheme 1

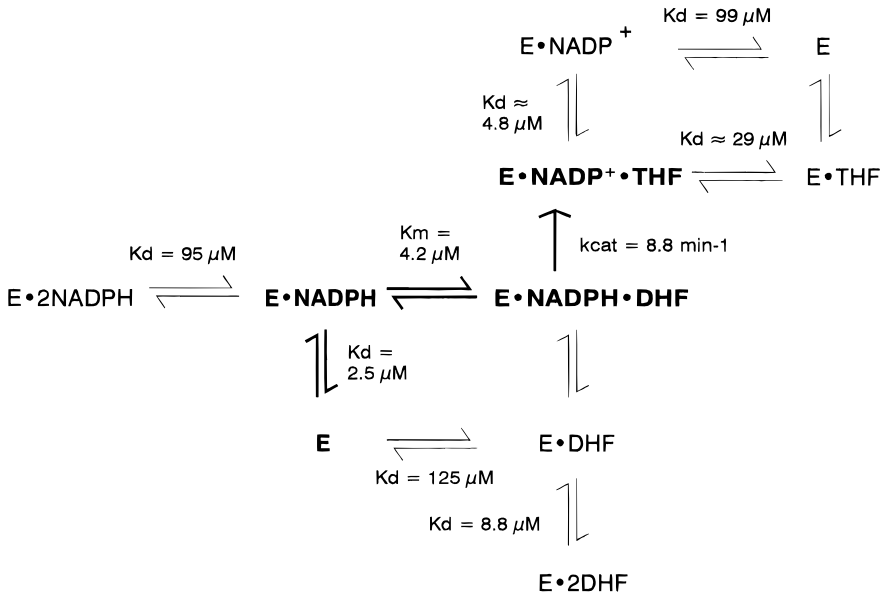

DHF (Table 2). This compares well with the second K_d for DHF binding under binary complex conditions (4.4 μM).

All the above results are consistent with binding a total of two ligands per tetramer, except for the binary $NADP^+$ complex. The observed stoichiometry of only 1 $NADP^+$ per tetramer indicates that either it binds differently enough from NADPH that a second $NADP^+$ molecule is sterically blocked from binding or that the positive charge prevents a second $NADP^+$ from binding. The latter seems more likely as under ternary complex conditions, either 1 DHF can bind to a 1:1 mixture of **R67** DHFR + $NADP^+$ or 1 $NADP^+$ can bind to a 1:1 mixture of **R67** DHFR + NADPH for a total of two ligands bound.

Comparison of Fluorescence and ITC Titrations. The stoichiometry determined by fluorescence and ITC agrees for the DHF binary complex; for folate, saturation was not reached for the fluorescence data, consistent with a weak initial binding of one folate molecule; and for $NADP^+$ there is no fluorescence experimental observable (Tables 1 and 2). The only major difference in binary binding stoichiometry occurs in the NADPH titrations. ITC data yields a stoichiometry of 1.56, whereas fluorescence yields 0.8. A possible complication with the fluorescence titration is that as two NADPH enter the active site pore, fluorescence energy-transfer between two bound NADPH's (homotransfer) could occur. This could result in a transfer depolarization term which could easily be misinterpreted in terms of a small amount of free NADPH, yielding the observed decrease in anisotropy at a stoichiometry of 0.8 (Figure 2B).

The ternary complex titrations using fluorescence and ITC also agree where there is a fluorescence signal to follow. One possible exception is the titration of NADPH into a 1:3 mixture of **R67** DHFR and folate, as monitored by fluorescence. However since a 1:3 mixture of **R67** DHFR and folate is not a saturating condition, a mixture of enzyme species is likely to be present initially. Addition of NADPH could occur to apo enzyme or **R67** DHFR·folate. An alternate interpretation might be binding of NADPH to a 1:2 complex of **R67** DHFR·folate for a total of three ligands bound. However, from the isothermal titration calorimetry data as well as the proposed cooperativity between heteroligands, it appears more likely that increasing concentrations of NADPH would displace bound folate from **R67** DHFR·2 folate and that the final species is a 1:1:1 complex of **R67** DHFR:folate:NADPH.

Correlation of Binding Results with Inhibition Studies. The above binding results are consistent with inhibition patterns observed by Morrison and Sneddon (1990). They found that N10 propargyl-5,8-dideazafolate (CB3717) displays parabolic competitive inhibition with respect to DHF binding (subsaturating NADPH conditions). Parabolic inhibition indicates binding of ≥two ligands (Segal, 1975). CB3717 becomes a normal competitive inhibitor of DHF under saturating NADPH conditions (Morrison & Sneddon, 1990), indicating binding of only one CB3717 per tetramer. In other words, two DHF binding sites are readily available at low NADPH concentrations, thus parabolic inhibition by CB3717 is observed. However, at higher NADPH concentrations, one DHF site is no longer accessible due to binding of one NADPH, thus CB3717 becomes a simple linear competitive inhibitor. These inhibition patterns are consistent with displacement of CB3717 by NADPH under saturating NADPH conditions. Displacement is not due to direct competitive inhibition but rather due to competition of NADPH and CB3717 for their respective binding sites in the **R67** DHFR half-pore. Whether an overlap exists between the folate and NADPH sites is not clear as co-crystals with NADPH have not been obtained.

Model for Binding and Catalysis. A model describing binding and catalysis is proposed in Scheme 1. All the DHF, NADPH, and $NADP^+$ binary K_d values were measured directly by ITC. To describe binding of DHF to **R67** DHFR·NADPH, the K_m for DHF was measured at pH 8.0. Binding constants for the reaction product, tetrahydrofolate (THF), were not measured directly as THF is not very stable. Instead the K_d for DHF binding to E·$NADP^+$ (Table 2) was used as an estimate for THF binding to E·$NADP^+$. Also for $NADP^+$, the K_i was used to estimate the K_d for $NADP^+$ binding to E·THF.

While binding of NADPH and DHF might be initially expected to follow a random addition mechanism, both the positive and negative cooperativity observed serve to establish a productive catalytic pathway from E to E·NADPH to E·NADPH·DHF to E·$NADP^+$·THF (shown in bold in

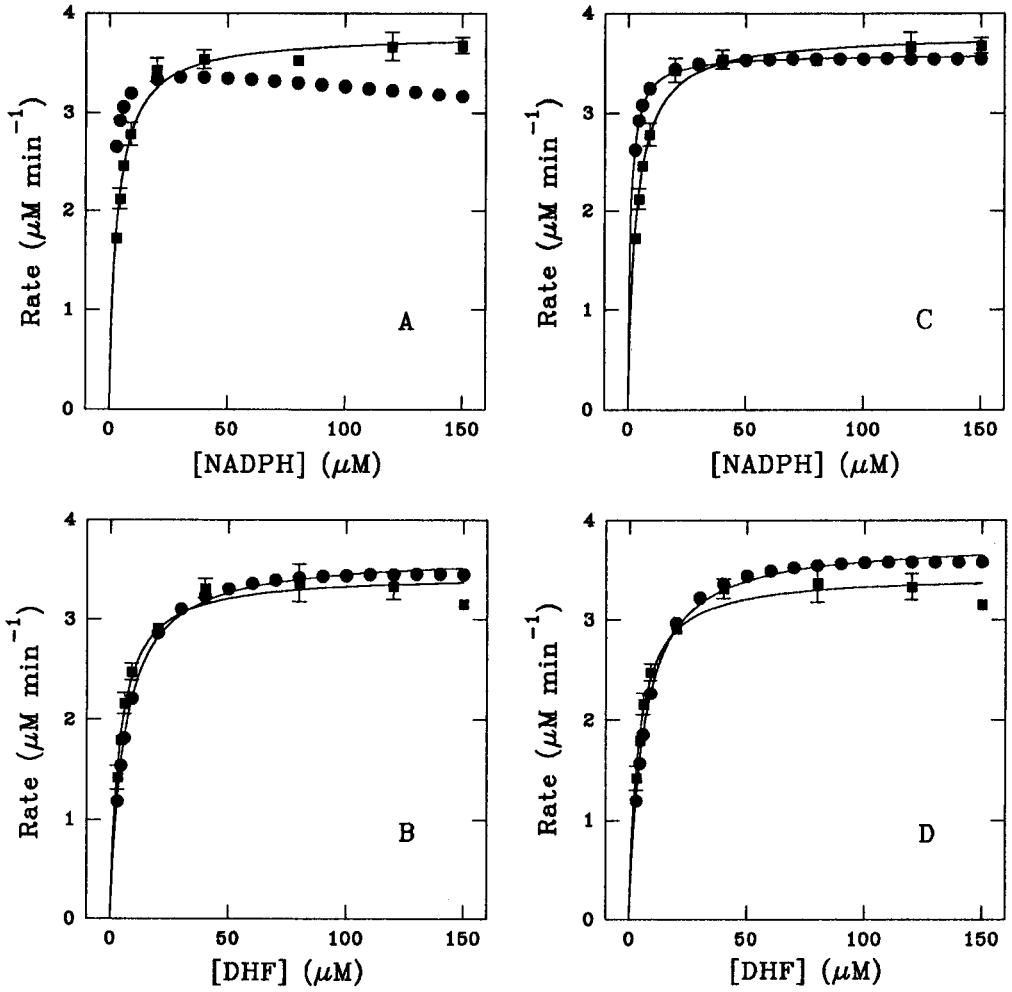

FIGURE 9: Comparison of experimental kinetic measurements (■) with KINSIM simulations (●), presented as substrate vs velocity plots. Measurements and simulations were carried out at an **R67** DHFR tetramer concentration of 0.43 μM. The kinetic measurements were carried out at 28 °C, as described in the Materials and Methods section. This is also the temperature at which the ITC measurements were made which yielded the K_d values used in the simulations. The error bars show the standard deviations in the experimental rates. Panels A and B compare the experimental results with the predictions of Scheme 1, while panels C and D compare experiment with the predictions of a related scheme that is described in the text. The fitted lines for the experimental and simulated data were generated by a fit to the Michaelis−Menten equation. Since the simulated data in panel A display obvious cofactor inhibition, no fit is shown.

Scheme 1). Cofactor inhibition is not observed under typical assay conditions as binding of a second NADPH requires a macroscopic K_d of 96 μM. Conversely, substrate inhibition is not observed as binding of the first DHF molecule requires a K_d of 250 μM; thus binding of the second DHF molecule and dead-end complex formation are minimized. If the K_d values for E ⇄ E·NADPH and E ⇄ E·DHF are combined with a K_m of 8 μM for DHF, then a K_d of 120 nM can be calculated for the addition of NADPH to E·DHF forming E·DHF·NADPH. This very tight binding would also effectively channel the binding pathway into productive catalysis. We have recently constructed a Q67H mutant **R67** DHFR and observe an approximately 60-fold decrease in both NADPH K_d values as well as a 200-fold decrease in DHF K_d values. This mutant clearly displays both substrate and cofactor inhibition (Park *et al.*, manuscript in preparation).

KINSIM, a kinetics modeling program (Barshop *et al.*, 1983), was used to model the mechanism proposed in Scheme 1 and simulate initial rate data. Figure 9A shows calculated substrate vs velocity plots for Scheme 1 as well as actual experimental data. Cofactor inhibition is predicted when only 20−30 μM NADPH is present. In practice, even higher levels of cofactor would be required to observe inhibition due to the error limit of the kinetic data (typically <10%). Since Scheme 1 predicts cofactor inhibition that is not observed in the experimental substrate vs velocity plots, a simulation was performed where the K_d for NADPH addition to E·NADPH to yield E·2NADPH was increased to 200 μM. In this simulation, NADPH inhibition was decreased enough so that it could be ascribed to experimental error (simulation not shown).

A second, related scheme was also considered since using the observed K_d of 96 μM for NADPH during the KINSIM simulation predicted cofactor inhibition. In this related scheme (not shown), the second NADPH molecule binds poorly in a symmetry related site due to ligand−ligand interactions. The ligand−ligand interactions concurrently serve to weaken the K_d for the first NADPH site. In this related scheme, loss of NADPH from E·2NADPH (K_d = 95 μM) results in E·NADPH′, which can then either lose NADPH to yield E (K_d = 95 μM) or isomerize to E·NADPH, where NADPH is bound more tightly. This interpretation is also supported by binding data from a mutant Q67H **R67** DHFR as this mutation affects both NADPH K_d values equally (Park *et al.*, manuscript in preparation). The predicted substrate vs velocity plots for this related scheme are shown in Figure 9C and D. Little to no substrate/cofactor

inhibition is predicted, in agreement with experimental data. Since either Scheme 1, with a higher K_d for the second NADPH site, or this related scheme predicts the steady state kinetic data fairly well, it is difficult to choose between the two. And except for this question concerning NADPH binding, the overall binding scheme predicts the steady state data well.

The K_d values for THF and $NADP^+$ binding were varied by factors of 2 in the simulations, and the predicted rates were not affected. While THF binding might also be expected to display a stoichiometry of 2, we did not explicitly enter this into the schemes as direct binding constants were not obtained and little THF would be expected to be present during initial rate studies.

Comparison of DHFRs. A recent article by Stephen Jay Gould (1995) points out that less complex does not necessarily mean more primitive. It may simply mean different and unrelated. This argument may perhaps be applied during comparisons of chromosomal and **R67** DHFRs. For example, *E. coli* chromosomal DHFR has been designated a highly evolved enzyme with a calculated efficiency of 0.15 (Fierke *et al.*, 1987). Recent *ab initio* quantum mechanical calculations suggest protein mediated electronic polarization of bound DHF and NADPH in *E. coli* DHFR may help lower energy barriers and aid catalytic function (Bajorath *et al.*, 1991a−c). Further, an overlap between the binding sites for $NADP^+$ and 5-deazafolate in human DHFR has been proposed to facilitate catalysis by compressing the distance between C6 of DHF and C4 of NADPH to a separation that is optimal for hydride transfer (Davies *et al.*, 1990).

Since **R67** DHFR has evolved recently in response to selective TMP pressure and it possesses an active site with a high degree of symmetry, it might be considered a model for a "primitive" enzyme (Narayana *et al.*, 1995). However, it readily circumvents the twin difficulties of binding two different substrates as well as substrate/cofactor inhibition. This is accomplished by binding NADPH and DHF differently (Narayana *et al.*, 1995) and then utilizing cooperativity to either minimize nonproductive binding of two identical substrates or to facilitate heteroligand interactions. This solution is quite different from that observed for chromosomal DHFRs and is correlated with the totally different tertiary and quaternary structures of the two DHFRs.

ACKNOWLEDGMENT

We thank Dave Matthews, Narendra Narayana, and Xuong Nguyen-huu for sharing their coordinates for dimeric and tetrameric **R67** DHFR structures and Cynthia Peterson for the use of her isothermal titration calorimeter. We also thank Cynthia for her helpful discussions and reading of the manuscript.

REFERENCES

Arnone, A. (1972) *Nature 237*, 146−149.
Baccanari, D., Phillips, A., Smithe, S., Sinski, D., & Burchall, J. (1975) *Biochemistry 14*, 5267−5273.
Bains, G., & Freire, E. (1991) *Anal. Biochem. 192*, 203−206.
Bajorath, J., Kitson, D. H., Fitzgerald, G., Andzelm. J., Kraut, J., & Hagler, A. T. (1991a) *Proteins 9*, 217−224.
Bajorath, J., Kraut, J., Li, Z., Kitson, D. H., & Hagler, A. T. (1991b) *Proc. Natl. Acad. Sci. U.S.A. 88*, 6423−6426.
Bajorath, J., Li, Z., Fitzgerald, G., Kitson, D. H., Farnum, M., Fine, R. M., Kraut, J., & Hagler, A. T. (1991c) *Proteins 11*, 263−270.
Barshop, B. A., Wrenn, R. F., & Frieden, C. (1983) *Anal. Biochem. 130*, 134−145.
Beechem, J. M., Gratton, E., Ameloot, M., Knutson, J. R., & Brand, L. (1991) *Topics in Fluorescence Spectroscopy, Volume 2: Principles* (Lakowicz, J. R., Ed.) pp 241−305, Plenum Press, New York.
Blakley, R. L. (1960) *Nature 40*, 1684−1685.
Brito, R. M., Rudolph, F. B., & Rosevear, P. R. (1991) *Biochemistry 30*, 1461−1469.
Creighton, T. E. (1993) *Proteins: Structures and Molecular Properties*, 2nd ed., p 381, W. H. Freeman and Co., New York.
Davies, J. F., II, Delcamp, T. J., Prendergast, N. J., Ashford, V. A., Freisheim, J. H., & Kraut, J. (1990) *Biochemistry 29*, 9467−9479.
Ellis, K. J., & Morrison, J. F. (1982) *Methods Enzymol. 87*, 405−426.
Farnum, M. F., Magde, D., Howell, E. E., Hirai, J. T., Warren, M. S., Grimsley, J. K., & Kraut, J. (1991) *Biochemistry 30*, 11567−11579.
Fierke, C. A., Kuchta, R. D., Johnson, K. A., & Benkovic, S. J. (1987) *Cold Spring Harbor Symp. Quant. Biol. 52*, 631−638.
Gornall, A. G., Bardawill, C. J., & David, M. M. (1949) *J. Biol. Chem. 177*, 751−766.
Gould, S. J. (1995) *Nat. Hist. 104*, 14−23.
Hillcoat, B. L., & Blakley, R. L. (1966) *J. Biol. Chem. 241*, 2995−3001.
Horecker, B. L., & Kornberg, A. (1948) *J. Biol. Chem. 175*, 385−390.
Howell, E. E., Warren, M. S., Booth, C. L. J., Villafranca, J. E., & Kraut, J. (1987) *Biochemistry 26*, 8591−8598.
Jones, T. R., Calvert, A. H., Jackman, A. L., Brown, S. J., Jones, M., & Harrap, K. R. (1981) *Eur. J. Cancer 17*, 11−19.
Lin, L.-N., Mason, A. B., Woodworth, R. C., & Brandts, J. F. (1991) *Biochemistry 30*, 11660−11669.
Ludescher, R. D., Peting, L., Hudson, S., & Hudson, B. (1987) *Biophys. Chem. 28*, 59−75.
Matthews, D. A., Smith, S. L., Baccanari, D. P., Burchall, J. J., Oatley, S. J., & Kraut, J. (1986) *Biochemistry 25*, 4194−4204.
Merabet, E., & Ackers, G. K. (1995) *Biochemistry 34*, 8554−8563.
Morrison, J. F., & Sneddon, M. K. (1990) in *Chemistry and Biology of Pteridines, 1989* (Curtius, H. Ch., Ghisla, S., & Blau, N., Eds.) pp 728−733, Walter de Gruyter & Co., Berlin.
Narayana, N., Matthews, D. A., Howell, E. E., & Xuong, N.-H. (1995) *Nat. Struct. Biol. 2*, 1018−1025.
Reece, L. J., Nichols, R., Ogden, R. C., & Howell, E. E. (1991) *Biochemistry 30*, 10895−10904.
Runnels, L. W., & Scarlata, S. F. (1995) *Biophys. J. 69*, 1569−1583.
Segal, I. H. (1975) *Enzyme Kinetics*, pp 465−470, John Wiley & Sons, New York.
Uyeda, K., & Rabinowitz, J. C. (1963) *Anal. Biochem.* 6, 100−108.
Visser, A. A. W. G., & Van Hoek, A. (1981) *Photochem. Photobiol. 47*, 201−205.
Williams, E. A., & Morrison, J. F. (1992) *Biochemistry 31*, 6801−6811.
Wiseman, T., Williston, S., Brandts, J. F., & Lin, L.-N. (1989) *Anal. Biochem. 179*, 131−137.
Zhuang, P., Yin, M., Holland, J. C., Peterson, C. B., & Howell, E. E. (1993) *J. Biol. Chem. 268*, 22672−22679.

BI960205D